Supplement of: Sea Ice Albedo Bounded Data Assimilation and Its Impact on Modeling: A Regional Approach

Joseph F. Rotondo[1], Molly M. Wieringa[1,2], Cecilia M. Bitz[1], Robin Clancy[3], and Steven M. Cavallo[3]

[1]Department of Atmospheric and Climate Science, University of Washington, Seattle, Washington, USA
[2]Advanced Study Program, NSF National Center for Atmospheric Research, Boulder, Colorado, USA
[3]School of Meteorology, University of Oklahoma, Norman, Oklahoma, USA

1 Adaptive Inflation for Sea Ice DA in QCEFF

The introduction of a bounded DA scheme complicates the use of classical inflation techniques. In traditional ensemble DA, multiplicative inflation is often applied to artificially increase model spread, enhancing the ensemble's ability to capture observed variability (Anderson and Anderson, 1999). However, this approach becomes problematic when applied to bounded variables, which must remain within strict physical limits. For example, during the melt season, SIC within a grid cell can approach zero. When μ is near zero, inflating the spread by a factor intended for Gaussian distributions can produce ensemble members that fall below zero–an unphysical state–or expand the distribution in a way that still fails to include nearby observed values. If, after inflation, the observation still falls outside the ensemble's acceptable range (here defined as within $\pm 2\sigma$ of the mean), the DA framework may reject it as inconsistent with the model prior. This mismatch highlights the challenge of using symmetric inflation schemes for variables with hard physical bounds and skewed distributions near those bounds.

Observation rejections can also occur even when values are not near physical bounds. These rejections stem from insufficient ensemble spread rather than model limitations, especially during rapid changes when μ diverges from the true model-generated observation. This issue is especially common during the melt season, when fast transitions often associated with albedo feedback and driven by melt-ponding, refreezing, or snowfall introduce variability that bounded ensemble systems struggle to accommodate.

To address these challenges, we apply a temporally varying adaptive inflation scheme available in DART, which enforces a minimum model spread (El Gharamti, 2018). This scheme models inflation factors as inverse-gamma distributed random variables. Inflation values evolve over time alongside the ensemble state, with their means and variances updated based on observational input. In our implementation within the QCEFF (Quantile Conserving Ensemble Filter Framework), the adaptive inflation diverges from its original formulation. Rather than enforcing strict bounds through priors or hard constraints–as in traditional bounded inflation schemes–the QCEFF-compatible version emphasizes physical consistency and conservation across the ensemble. This reformulation decouples inflation from rigid statistical boundaries and instead aligns it with the QCEFF's diagnostic balance principles (Anderson, 2022, 2023).

This adaptive inflation framework ensures stability and consistency by preserving the integrity of the initial ensemble spread introduced during the spin-up phase. We fix the minimum inflation factor at 1.0, maintaining the original ensemble spread prior to data assimilation. The upper bound is set at 50.0, although this limit is rarely approached due to the physical constraints imposed by the bounded DA scheme. To regulate how inflation evolves over time, we constrain the standard deviation of the inverse gamma distribution used to sample the inflation factor. Specifically, the distribution's standard deviation must be no smaller than 0.6, ensuring a minimum level of ensemble variability, and the distribution's width is restricted such that the inflation standard deviation cannot grow or shrink by more than a factor of 1.05 per time step. These constraints, informed by

prior work (e.g., Wieringa et al., 2024), are designed to prevent overly abrupt changes in inflation while allowing sufficient flexibility to respond to dynamic error growth.

2 Sensitivity to Observational Noise Realizations

While generating synthetic observations, we applied random perturbations drawn from a specified distribution around the TRUTH state. This is standard practice in perfect-model assimilation experiments to simulate measurement uncertainty. In our case, observations were generated using the `perfect_model_obs` tool in DART, which employed the QCEFF with bounded, non-Gaussian likelihoods. These were configured through the `obs_error_info` table by prescribing physical bounds for each variable. As a result, the synthetic observations were sampled from piecewise-linear distributions consistent with the bounded likelihoods, rather than simple Gaussians.

Because this approach represents a relatively novel method for generating synthetic observations—particularly in sea ice data assimilation–we assessed whether variability in specific realizations of random noise could influence assimilation performance. We repeated a subset of six SIAL-only assimilation experiments under the medium uncertainty configuration, each using a distinct random seed to produce three separate realizations of observational noise (with identical error magnitude and statistical bounds). Root Mean Square Error (RMSE) was computed for SIC and SIT across all regions and ensemble truth members.

As shown in Figure S1, differences in RMSE across noise realizations were negligible, and the relative ordering of assimilation performance among experiments remained unchanged. This result is consistent with theoretical expectations: because all realizations are drawn from the same bounded likelihood defined in `obs_error_info`, and the same table is used during both observation generation and assimilation, the system remains statistically consistent. Moreover, the ensemble nature of the assimilation—using 30 members—and the high spatial and temporal observation density act to dampen the influence of any individual realization. Over many assimilation cycles, random fluctuations are averaged out, and the filter converges on similar solutions regardless of the specific noise pattern.

We further note that some minor variation could emerge during early cycles, when fewer observations have been assimilated and their influence is more localized. However, in long-term (many month) perfect-model experiments such as this one, where the system is well-observed and observations are generated in a self-consistent manner, the stochasticity of synthetic noise has limited impact. These findings reinforce the robustness of DART's QCEFF system for assimilating bounded, non-Gaussian observational errors in high-density sea ice observing systems.

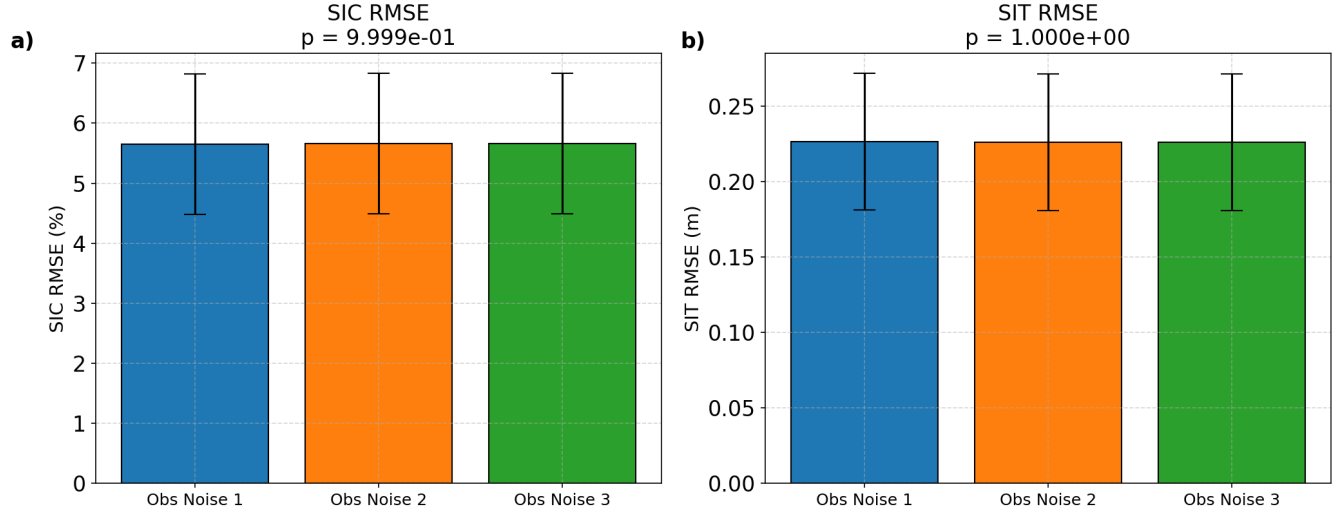

Figure S1. Impact of random observational noise on SIAL assimilation (medium uncertainty case) for SIC (a) and SIT (b) RMSEs, averaged across six ensemble truth members and all regions. Each of the three "Obs Noise" levels corresponds to a different random realization of observational noise with the same magnitude (2σ error). Error bars show 95% confidence intervals based on ensemble–region combinations. SIC cutoffs from Fig. S2 were utilized when calculating SIT RMSE. A one-way ANOVA was performed to test whether RMSE values significantly differ between noise realizations. The resulting p-values near 1.0 indicate no statistically significant difference across noise realizations, suggesting that the DA system effectively accounts for uncertainty generated from random noise. This result supports the robustness of DART's QCEFF to random perturbations when the observation error variance is correctly specified. The use of 30 ensemble members in the assimilation step likely contributes to this robustness, as the effects of random noise are averaged out across the ensemble.

3 SIAL P-Values for Comparison

Table S1: Statistical significance of SIAL RMSE comparisons ($p < 0.05$), based on Fig. 5. Comparisons not involving SIAL (e.g., SIT vs. Free Run) are excluded. Regions not shown indicate cases where no SIAL assimilation configurations were statistically distinguishable from other assimilation types.

Region	Comparison	p-value	Better Performer
SIC RMSE – SIAL Comparisons			
Barents	SIAL (Low Error) vs SIAL (Medium Error)	0.0055	SIAL (Low Error)
	SIAL (Low Error) vs SIAL (High Error)	0.0007	SIAL (Low Error)
	SIAL (Medium Error) vs SIAL (High Error)	0.0406	SIAL (Medium Error)
	SIAL (Low Error) vs SIC	0.0011	SIAL (Low Error)
	SIAL (Low Error) vs. SIT	0.0000	SIAL (Low Error)
	SIAL (Low Error) vs. Free Run	0.0000	SIAL (Low Error)
	SIAL (Medium Error) vs SIC	0.0059	SIAL (Medium Error)
	SIAL (Medium Error) vs. SIT	0.0000	SIAL (Medium Error)
	SIAL (Medium Error) vs. Free Run	0.0000	SIAL (Medium Error)
	SIAL (Medium Error) vs. All Variables	0.0091	All Variables
	SIAL (High Error) vs. SIT	0.0007	SIAL (High Error)
	SIAL (High Error) vs. Free Run	0.0000	SIAL (High Error)
	SIAL (High Error) vs. All Variables	0.0007	All Variables
CoastalCanada	SIAL (Low Error) vs SIT	0.0050	SIAL (Low Error)
	SIAL (Low Error) vs Free Run	0.0044	SIAL (Low Error)
	SIAL (Medium Error) vs SIT	0.0164	SIAL (Medium Error)
	SIAL (Medium Error) vs Free Run	0.0139	SIAL (Medium Error)
	SIAL (High Error) vs SIT	0.0231	SIAL (High Error)
	SIAL (High Error) vs Free Run	0.0194	SIAL (High Error)
SibChuk	SIAL (Low Error) vs SIAL (Medium Error)	0.0001	SIAL (Low Error)
	SIAL (Low Error) vs SIAL (High Error)	0.0003	SIAL (Low Error)
	SIAL (Low Error) vs SIT	0.0051	SIAL (Low Error)
	SIAL (Low Error) vs Free Run	0.0002	SIAL (Low Error)
	SIAL (Medium Error) vs SIC	0.0004	SIC
	SIAL (Medium Error) vs SIT	0.0069	SIT
	SIAL (Medium Error) vs All Variables	0.0001	All Variables
	SIAL (High Error) vs SIC	0.0011	SIC
	SIAL (High Error) vs SIT	0.0119	SIT
	SIAL (High Error) vs All Variables	0.0003	All Variables
SIT RMSE – SIAL Comparisons			
Barents	SIAL (Low Error) vs Free Run	0.0002	SIAL (Low Error)
	SIAL (Low Error) vs All Variables	0.0062	All Variables
	SIAL (Medium Error) vs Free Run	0.0004	SIAL (Medium Error)
	SIAL (Medium Error) vs All Variables	0.0030	All Variables
	SIAL (High Error) vs Free Run	0.0056	SIAL (High Error)
	SIAL (High Error) vs All Variables	0.0011	All Variables
SibChuk	SIAL (Low Error) vs SIAL (Medium Error)	0.0060	SIAL (Low Error)

Continued on next page

Table S1 (continued)

Region	Comparison	p-value	Better Performer
	SIAL (Low Error) vs SIAL (High Error)	0.0311	SIAL (Low Error)
	SIAL (Medium Error) vs SIT	0.0149	SIT
	SIAL (Medium Error) vs All Variables	0.0043	All Variables
	SIAL (High Error) vs All Variables	0.0233	All Variables

4 SIT RMSE Calculation

When calculating $SIT_{agg} = \frac{\sum_{n=1}^{n_{cat}=5} vice_n}{SIC_{agg}}$, a cutoff threshold on SIC is needed to prevent artificially inflated SIT uncertainties. The SIT_{agg} estimate often exhibits non-Gaussian behavior, including a heavy upper tail due to elevated $vice_n$ values despite low SIC_{agg} (Zhang et al., 2018).

To mitigate this issue, we iteratively examined the SIT RMSE distribution for each region under varying SIC cutoff thresholds. For each region, we selected the lowest SIC threshold at which the average RMSE slope across all assimilation experiments dropped below 0.01 ($m < 0.01$), thereby avoiding artificial inflation of SIT error. The resulting region-specific SIC cutoff values are summarized in Table S2. Corresponding SIT RMSE distribution plots for each threshold are provided in Figure S2.

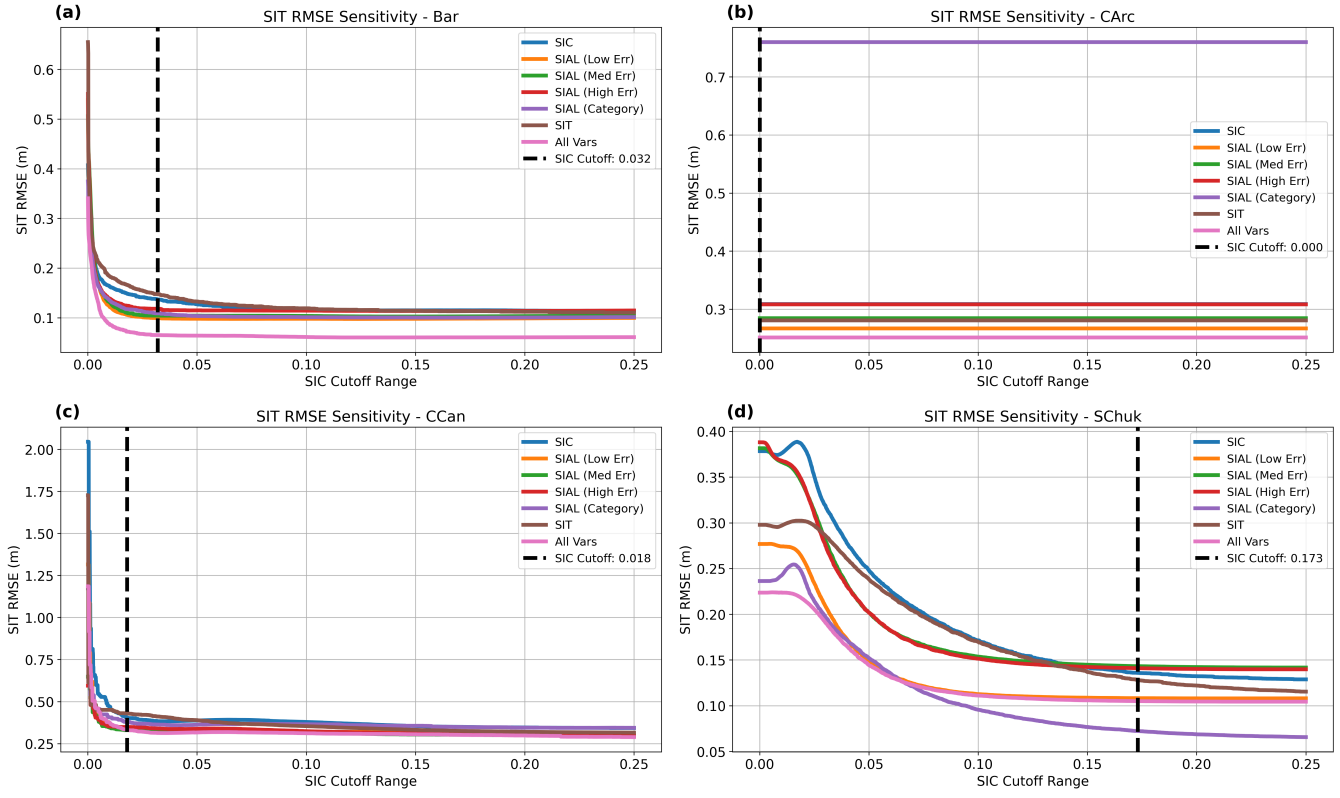

Figure S2. Sensitivity of SIT RMSE to SIC cutoff thresholds across four Arctic regions: Barents Sea (a), Central Arctic (b), Coastal Canada (c), and Siberian-Chukchi Sea (d). Each line represents a different assimilation experiment setup, including SIC-only, SIAL with varying uncertainty levels, SIT-only, and all variables combined. The SIC cutoff is defined as the first SIC threshold at which the average slope (m) of SIT RMSE with respect to increasing SIC cutoff is less than 0.01. Vertical dashed lines indicate these cutoff points, expressed as fractional SIC values: 0.032 (Barents Sea), 0.000 (Central Arctic), 0.018 (Coastal Canada), and 0.173 (Siberian-Chukchi Sea).

Table S2. SIC cutoff percentages by region, based on the first location where the average $m < 0.01$.

Region	**SIC Cutoff (%)**
Barents Sea	3.2
Central Arctic	0.0
Coastal Canada	1.8
Siberian-Chukchi Sea	17.3